

Grain refinement due to complex twin formation in rapid hot forging of magnesium alloy

Yunping Li,^{a,*} Shuo Wu,^a Huakang Bian,^b Ning Tang,^b Bin Liu,^c Yuichiro Koizumi^a and Akihiko Chiba^a

^a*Institute for Materials Research, Tohoku University, Sendai 980-8577, Japan*

^b*Graduate School of Engineering, Tohoku University, Sendai 980-8577, Japan*

^c*State Key Lab for Powder Metallurgy, Central South University, Changsha, Hunan, People's Republic of China*

Received 19 May 2012; revised 10 September 2012; accepted 8 October 2012

Available online 16 October 2012

Twinning behavior and twin interactions were investigated to characterize grain refinement in magnesium alloys subjected to rapid hot forging. Formation of $\{10\bar{1}2\}$ tensile twins with various twin variants and their subsequent mutual interaction resulted in new boundaries at low strain. With further straining, fragmentation of $\{10\bar{1}1\}$ - $\{10\bar{1}2\}$ double twin bands by the formation of more complex twins in the interior, accompanied by a drastic decrease in the stored energy, led to grain refinement. Crown Copyright © 2012 Published by Elsevier Ltd. on behalf of Acta Materialia Inc. All rights reserved.

Keywords: Magnesium alloy; Grain refinement; Hot forging; Twinning

Numerous studies have shown that the grain refinement occurring during hot working of Mg alloys is closely related to twinning activity [1–6], which is especially obvious in low-temperature and/or high-strain-rate regimes where twinning becomes the dominant deformation mechanism [4–6]. Dynamic recrystallization (DRX) of Mg alloy has been investigated under conditions of warm deformation by Yin et al. [4], and at room temperature (RT) by Kelley et al. [1] in which the nucleation of new grains through DRX, driven by the distortion energy accumulated from twinning was reported. The influence of twinning on grain refinement in AZ31B alloys was analyzed by Yu et al. [5] by studying a combination of the refined grain size with and without the influence of twinning, along with the Zener–Hollomon (Z) parameter; they found that twinning favors the formation of finer grains. Recently, Ma et al. [6] suggested the idea of twin-induced grain refinement using electron backscatter diffraction (EBSD) analysis, which is conceptually different from that proposed by Yin et al. [4]. Ma et al. found that a large number of refined grains were surrounded by rough and incoherent $\{10\bar{1}2\}$ tensile twin boundaries, which were gradually rotated into general grain boundaries by external stress.

However, Ma et al. ascribed the refining mechanism to the $\{10\bar{1}2\}$ tensile twin formation, although prominent misorientation angle distribution peaks also appeared at about 30° and 38° , which are generally related to the $\{10\bar{1}1\}$ - $\{10\bar{1}2\}$ double twins as mentioned in a number of earlier reports [4,5]. It is well known that the $\{10\bar{1}2\}$ tensile twin is usually formed extensively at low strains owing to the low critical resolved shear stress (CRSS) required and is prone to disruption by subsequent deformation or to coalescence with further straining [7]. In order to quantitatively investigate twinning-related grain refinement under hot working, extensive research on the behaviors of tensile $\{10\bar{1}2\}$ and other twins, the roles of these twins in the formation of new grain boundaries, and the orientation relationship between the twins and refined grains are required. However, few reports have addressed these aspects specifically. Hence, in this work, we analyzed by EBSD: (i) the twinning behavior, (ii) the twin interactions; and (iii) the specific orientation relationship between the new grains and the twins at various strain levels in AZ31B Mg alloys subjected to rapid hot forging. The results of our study revealed an interesting grain-refinement mechanism.

Cylindrical samples of AZ31 alloy (8 mm diameter \times 12 mm high) were cut from an extruded rod. Compressive tests were carried out along the extrusion

*Corresponding author. Tel.: +81 22 215 2452; fax: +81 22 215 2116; e-mail: lyping@imr.tohoku.ac.jp

direction (ED) in vacuum at 250 °C using a computer-aided Thermecmaster-Z hot-forging simulator. The strain rate used was 10 s^{-1} . The specimens were heated to the target temperature at a rate of 5 °C s^{-1} by high-frequency induction. As soon as the samples had been compressed to the final strain level, they were quenched to RT with He (4 MPa). Analysis of the microstructure was carried out at the center of the compressed samples by EBSD, using data acquisition software (TSL-OIM 5.0). Textures of the samples were scanned by the EBSD equipment over a fixed area ($200 \mu\text{m} \times 130 \mu\text{m}$) with a step size of $0.35 \mu\text{m}$.

To analyze the grain- and twin-boundary evolution with respect to strain, misorientation angle distributions at various strain levels were analyzed by EBSD, as shown in Figure 1. Only boundaries with misorientation angles $>5^\circ$ were considered in the current study, because the boundary angles $<5^\circ$ measured by EBSD were observed to be drastically affected by the polishing state compared to the boundaries with higher angles. Rotation axis distributions of some of the prominent peaks are inserted in the corresponding figures. The as-received sample exhibited a random distribution of misorientation angles, without a dominant rotation axis (Fig. 1a). In the deformed sample, distinguished boundary misorientation peaks in the ranges $5\text{--}10^\circ$, $29\text{--}31^\circ$, $37\text{--}39^\circ$, $53\text{--}61^\circ$ and $86\text{--}88^\circ$ about the $\langle 2\bar{1}\bar{1}0 \rangle$ axis; $29\text{--}31^\circ$ about the $\langle 0001 \rangle$ axis; and $53\text{--}61^\circ$ about the $\langle 10\bar{1}0 \rangle$ axis were observed. For the specimens deformed to a true strain of 0.08, a maximum peak range of the boundary misorientation existed around $86\text{--}88^\circ$ about the $\langle 2\bar{1}\bar{1}0 \rangle$ axis, and the other peaks were much weaker. With the increase in strain, the maximum peak range shifted from $86\text{--}88^\circ/\langle 2\bar{1}\bar{1}0 \rangle$ to the other peaks. After straining to ~ 0.15 , the frequencies of the boundary misorientation peaks around $29\text{--}31^\circ$, $37\text{--}39^\circ$ and $53\text{--}61^\circ$ increased to their maximum values (Fig. 1c). The boundary misorientation gradually became ran-

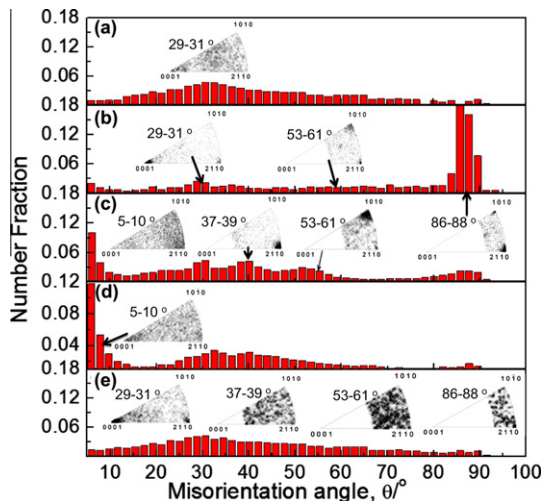


Figure 1. Number fractions of the misorientation angle in AZ31 Mg alloy. Misorientation axis distributions in the crystal coordinate system are shown for some significant angular ranges for (a) as-received samples and for samples deformed to true strains of (b) 0.08, (c) 0.15, (d) 0.4 and (e) 0.7.

domly distributed at a strain of 0.7 (Fig. 1d, e). Most of the peaks that occurred at lower strains disappeared at a strain of 0.7 (Fig. 1e), and no noticeable rotation axis in the above-mentioned angular ranges were detected, except for the rotation angle around $29\text{--}31^\circ$, where the two rotation axes ($\langle 0001 \rangle$ and $\langle 2\bar{1}\bar{1}0 \rangle$) were still significantly prominent.

Combining the rotation axis distributions obtained at various strains and the previously reported results [8], it was confirmed that the local peak in the range $86\text{--}88^\circ$ about the $\langle 2\bar{1}\bar{1}0 \rangle$ axis can be ascribed to the $\{10\bar{1}2\}/\{10\bar{1}0\}$ tensile twin. In addition, the peaks around $5\text{--}10^\circ/\langle 2\bar{1}\bar{1}0 \rangle$ and $53\text{--}61^\circ/\langle 10\bar{1}0 \rangle$ boundaries were found to be related to two separate $\{10\bar{1}2\}$ twins ($\{10\bar{1}2\}/\{10\bar{1}2\}$) with various twin variants [8]. Also, both the peaks around $29\text{--}31^\circ/\langle 2\bar{1}\bar{1}0 \rangle$ and around $37\text{--}39^\circ/\langle 2\bar{1}\bar{1}0 \rangle$ boundaries were generated from the $\{10\bar{1}1\}/\{10\bar{1}2\}$ double twins [9]. The peak around the $53\text{--}61^\circ/\langle 2\bar{1}\bar{1}0 \rangle$ boundary was formed because of the $\{10\bar{1}1\}/\{10\bar{1}0\}$ compressive twin [8]. A preference for $\langle 0001 \rangle$ was also observed in the rotation angle range $29\text{--}31^\circ$ (Fig. 1b–e) throughout the deformation. However, it was not confirmed theoretically whether this was related to the twins or slips. From the above results, it can be inferred that by increasing strain to ~ 0.15 , the misorientation peak for the $\{10\bar{1}2\}$ twins increased to their maximum value at a strain of ~ 0.08 , and vanished gradually. This was accompanied by the strengthening of some peaks such as those at the $5\text{--}10^\circ/\langle 2\bar{1}\bar{1}0 \rangle$ and $53\text{--}61^\circ/\langle 10\bar{1}0 \rangle$ boundaries, due to the interaction between the $\{10\bar{1}2\}$ twin boundaries with various twinning variants (Fig. 1a–e).

Figure 2a illustrates the microstructure after slight compression (to a strain of 0.08) in terms of the inverse

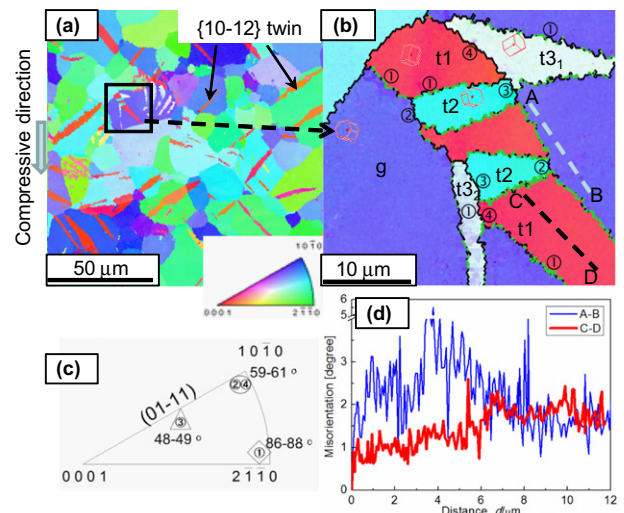


Figure 2. (a) Inverse pole figure map of the AZ31B alloy after hot compression to a true strain of 0.01. (b) A magnified image of the rectangular region represented in (a), indicating the formation of various kinds of boundaries by the interaction of $\{10\bar{1}2\}$ tensile twins with various twin variants, in which compression direction is parallel to ED. (c) Schematic misorientation axis distribution of the new boundaries formed by the interaction of $\{10\bar{1}2\}$ tensile twins with various twin variants. (d) Point-to-origin profiles along the straight lines A–B and C–D represented in (b).

Download English Version:

<https://daneshyari.com/en/article/1498867>

Download Persian Version:

<https://daneshyari.com/article/1498867>

[Daneshyari.com](https://daneshyari.com)